Supplemental Figure Legends

Supplementary Figure 1. Formation of core-duct and DB states during late gestation. (A,B) Plexus-to-duct transformation (from Fig. 2I,L) showing plexus (blue dashed line in *A*) connected to duct (yellow dashed line in *B*). Sox9 in plexus and duct-states (*C* is sectional inset from *B*). (D,E) Analysis of nuclear position and shape in plexus versus core duct states. (F) Quantification of mean fluorescence intensities in $Sox9^{+}$ populations from plexus and duct states at E17.5 (G,J) Epifluorescence images of 30-40 μm-thick cryosections showing central (red dashed line) and interlobular ducts (green dashed line) at E17.5. (H,I,K,L) Fluorescence detection of DBA^{+}, $Muc1^{+}$, and $CK19^{+}$ epithelium at 40x magnification in ~35 μm confocal z-stacks. DBA marks the central (yellow arrow), interlobular (yellow arrowhead), and intralobular ducts (blue arrow). (L) CK19 marks the same, in addition to DBA^{-} intercalating ducts (blue arrowhead). Scale bars are 15 μm in *A-C*, 100 μm in *G,K*; 20 μm in *H,I,K,L*.

Supplementary Figure 2. Dynamics of plexus-to-duct transformation in the core. Measurement of relative pixel area for $Muc1^{+}$ plexus over the combined plexus and duct-state pixel area in the core. Measurements were taken from serial 30-40 μm thick sections covering whole dorsal pancreata. Measurements exclude $Muc1^{+}$ ductal branches and pro-acinar tips. Measurements were taken using ImageJ software. Error bars are S.E.M, n = 3 for each time point.

Supplementary Figure 3. The Ngn3 to Sox9 ratio indicates the balance between endocrine differentiation and progenitor maintenance. (A) Lineage diagram showing the progression, from replicating $Sox9^{+}$ progenitor status, through sequential $Ngn3^{+}$ states during endocrine-lineage commitment. Ngn3 and Sox9 co-expression in the epithelium ($Sox9^{+}Ngn3^{+}$) defines the initial $Ngn3^{+}$ state, followed by high levels of Ngn3 during delamination ($Sox9^{-}Ngn3^{HI}$), and finally Ngn3 down-regulation ($Sox9^{-}Ngn3^{LO}$) in committed endocrine cells. (B-D) Derivation of endocrine yield, a quantitative descriptor of endocrine-lineage flux from the epithelium, based on a measured ratio of

Ngn3^{+} and Sox9^{+} cell states. (B) Theoretical segment of the trunk-epithelium with a representative distribution of Sox9^{+} and Ngn3^{+} cell states. (C) The Ngn3:Sox9 ratio observed at a given sampling time is determined by the temporal relationship between the Sox9^{+} cell-cycle period (growth parameter) and the duration of the Ngn3-positive period of endocrine commitment (differentiation parameter). (D) Provided comparable time-frames for these two parameters, endocrine yield can be determined by converting the Ngn3:Sox9 ratio into a fractional representation reflecting the number of cells maintaining replicative Sox9^{+} cell status, versus differentiating Ngn3^{+} status, in a defined epithelial segment at a given time.

Supplementary Table 1. Absolute numbers of Sox9^{+} mitotic figures and Ngn3^{+} cells states evaluated at each time point during EdU pulse-chase time-course analyses. "n" indicates the number of pancreata sampled for each time point.

Supplementary Figure 4. Ngn3 is down-regulated before acquisition of Pdx1^{HI} status. (A-F) Immuno-detection of Ngn3 and Pdx1 in cryosections at indicated stages. The vast majority of Ngn3^{+} cells co-express low levels of Pdx1 (white arrowheads). Low levels of Pdx1 are also observed in the Ngn3^{-} epithelium (yellow arrowheads in *C,F*). Pdx1^{HI} cells do not co-express Ngn3 (blue arrowheads). Scale bars are 20 μm.

Supplementary Figure 5. New Ngn3^{+} cells are generated throughout 2^{O} transition. Proportion of the total Ngn3^{+} population that is positive for Sox9 (early Ngn3^{+}Sox9^{+} cell state) at indicated stages. Error bars are S.E.M for n = 3 pancreata at each stage, 30% of total pancreas scored. No statistical difference was detected at any stage ($p = 0.5912$, one-way Anova).

Supplementary Figure 6. Ngn3^{+} and Sox9^{+} immune-detection indicates robust endocrine differentiation throughout the 2^{O} transition. (A-L) Representative images of Sox9^{+} and Ngn3^{+} populations at stages

indicated. Later stage (E16-17.5) images focus on epithelium where $Ngn3^+$ cells are being born in large numbers. Scale bars are 50 μm.

Supplementary Figure 7. $Sox9^+$ populations mark plexus, duct, and ductal-branch states. (A-F) Whole mount z-stack reconstructions of Sox9 and Muc1-labeled epithelium in peripheral segments of wild-type dorsal pancreas at E14.5 and E17.5. Blue, red, and green boundaries demarcate plexus, duct, and ductal-branch states, respectively. (C,F) Pro-acinar tips are demarcated by intense Muc1 signal, a bulb-like morphology that becomes clefted and elongated over time, and a low nuclear Sox9 signal that diminishes over time. Scale bars are 20 μm.

Supplemental Figure 8. Endocrine differentiation in the plexus-state persists late into 2^O transition. (A-D) Muc1, Ngn3, and Sox9 whole-mount immunolabeling of core and peripheral regions of dorsal pancreas exhibiting plexus (blue dashed line), ductal-branch (green dashed line), and duct (red dashed line) states at E18.5. Note reduced Sox9 levels in duct compared to plexus in *B*. Scale bars are 20 μm.

Supplementary Figure 9. Epithelial Hes1-production is reduced under *Ngn3*-deficient conditions. (A-D) Frozen section analysis of the ratios of $Hes1^+$ and $Sox9^+$ populations in the trunk domain of control and *Ngn3*-deficient animals. (D) Blue arrowheads indicate clusters of $Hes1^+$ cells in the $Ngn3^{EGFP/EGFP}$ samples.

Supplementary Figure 10. S-phase indices in acinar cells are unchanged in *Ngn3*-deficient pancreata. (A) Representative 20x image of EdU incorporation at 1 hour post-injection in $amylase^+$ acinar clusters of $Ngn3^{EGFP/+}$ and $Ngn3^{EGFP/EGFP}$ dorsal pancreas. (B) Quantification of the Edu-incorporation index. Scale bars are 50 μm. Error bars are S.E.M. N = 1673 $Ngn3^{EGFP/+}$ and N = 1436 $Ngn3^{EGFP/EGFP}$ $amylase^+$ cells counted from five sections spanning n = 2 dorsal pancreas for each genotype.

Supplementary Figure 11. Late-stage corrective remodeling in Ngn3-deficient epithelium. Muc1 and insulin labeling in 40 μm thick sections showing representative core (A-L) and peripheral (M & N) regions

of *Ngn3*$^{EGFP/+}$ and *Ngn3*$^{EGFP/EGFP}$ pancreata at stages indicated. Scale bars are 30 μm in A,D,G-L; 20 μm in B,E; 50 μm in C,F; 100 μm in M,N.

Supplementary Figure 12. Feedback control of endocrine progenitor growth, differentiation, and morphogenesis in the plexus niche. (*A*) Diagrammatic representation of the principle morphogenetic processes comprising trunk epithelial morphogenesis during 2^{O} transition. Regions of the organ enriched for Notch-responsive endocrine progenitors are demarcated in blue, whereas regions reduced or absent in this respect are orange. Diagram intends to contrast the extremes of each morphological state and process, with only rough anatomical precision. (*B*) Diagrammatic representation of the local feedback interactions operating in the plexus-state.

Supplementary Table 2. Antibodies and Detection Methods.

Supplementary Table 3. Primers used for genotyping and qPCR analyses

Bankaitis_Supp. Fig1

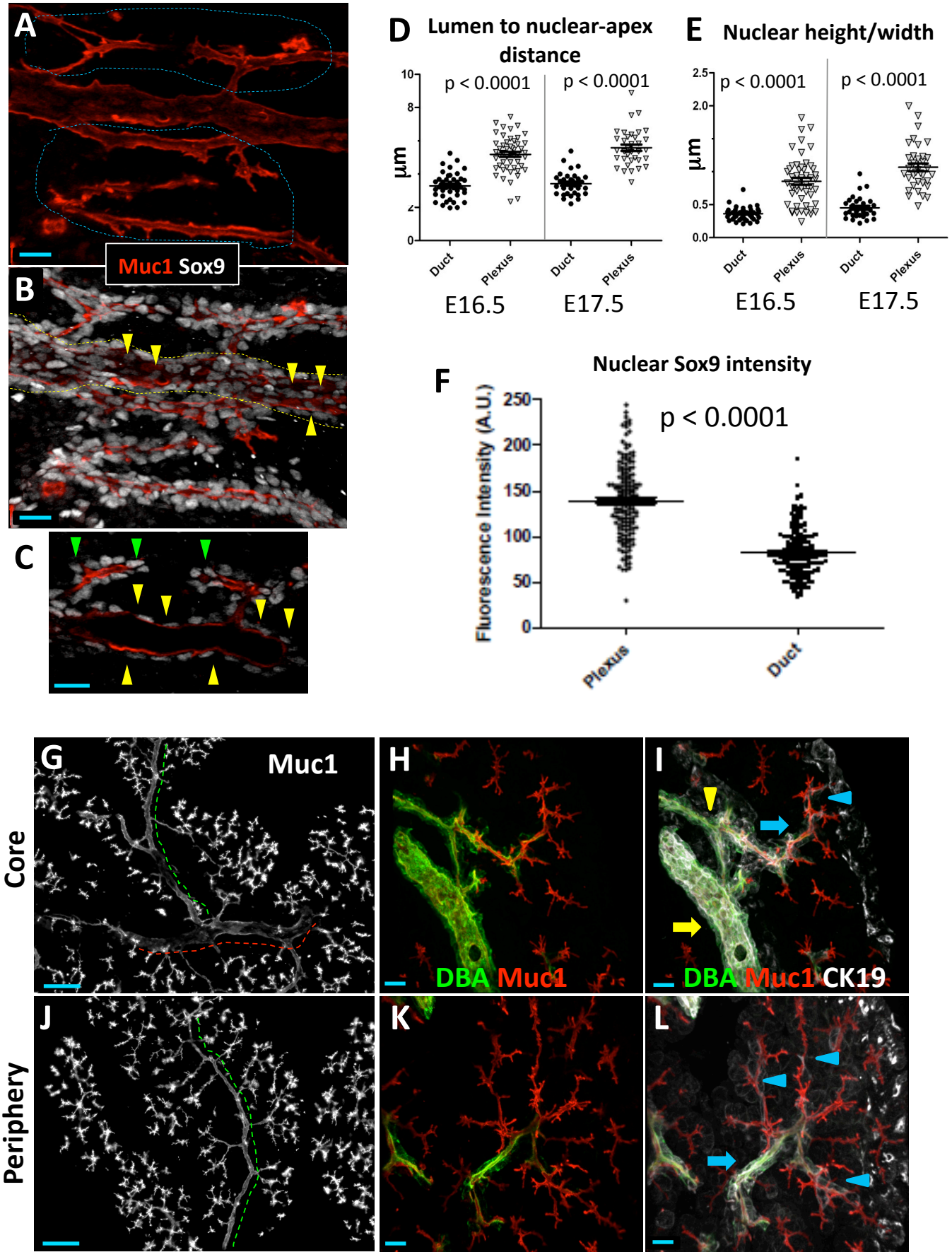

Bankaitis_Supp. Fig2

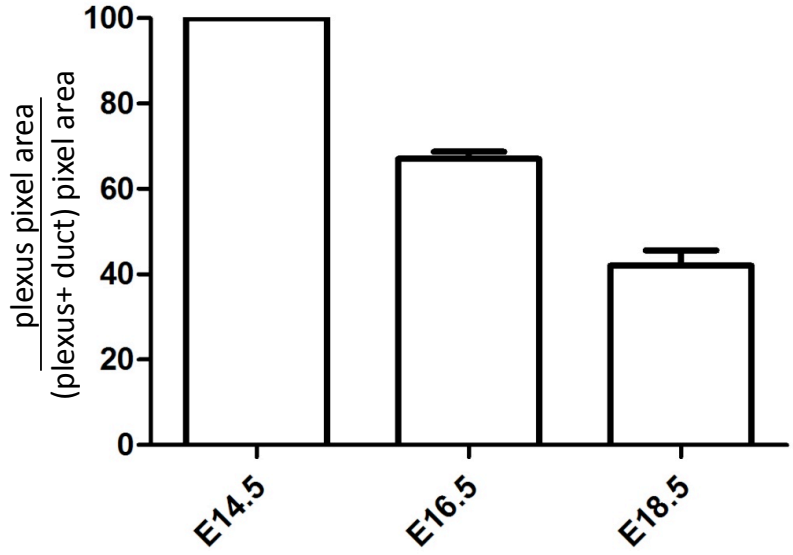

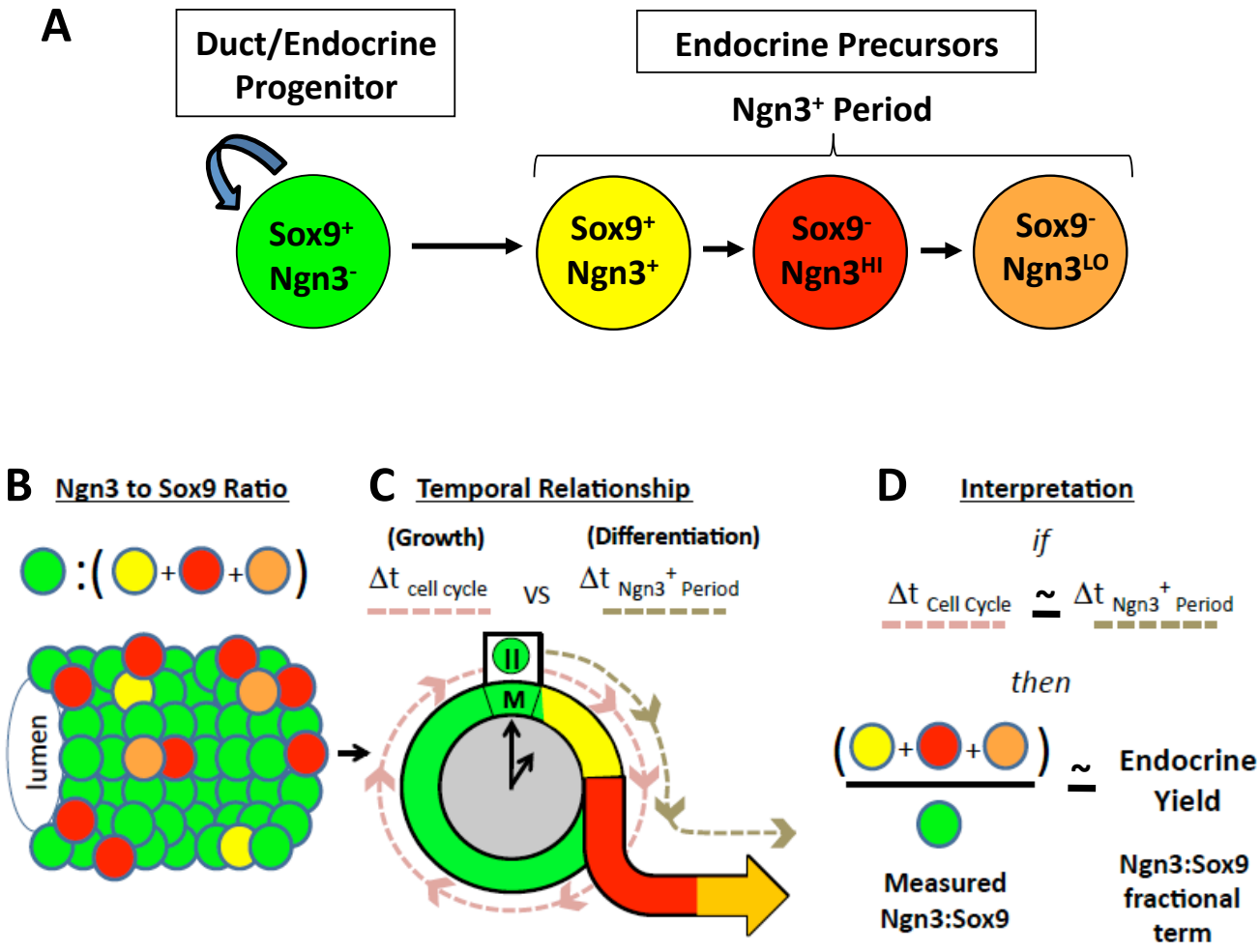
A
Duct/Endocrine Progenitor
Endocrine Precursors
Ngn3+ Period
Sox9+ Ngn3-
Sox9+ Ngn3+
Sox9- Ngn3HI
Sox9- Ngn3LO
B Ngn3 to Sox9 Ratio
lumen
C Temporal Relationship
(Growth)
(Differentiation)
Δt cell cycle
VS
Δt Ngn3+ Period
G1
M
D Interpretation
if
Δt Cell Cycle ≃ Δt Ngn3+ Period
then
≃
Endocrine Yield
Measured Ngn3:Sox9
Ngn3:Sox9 fractional term

Bankaitis_Supp. Fig4

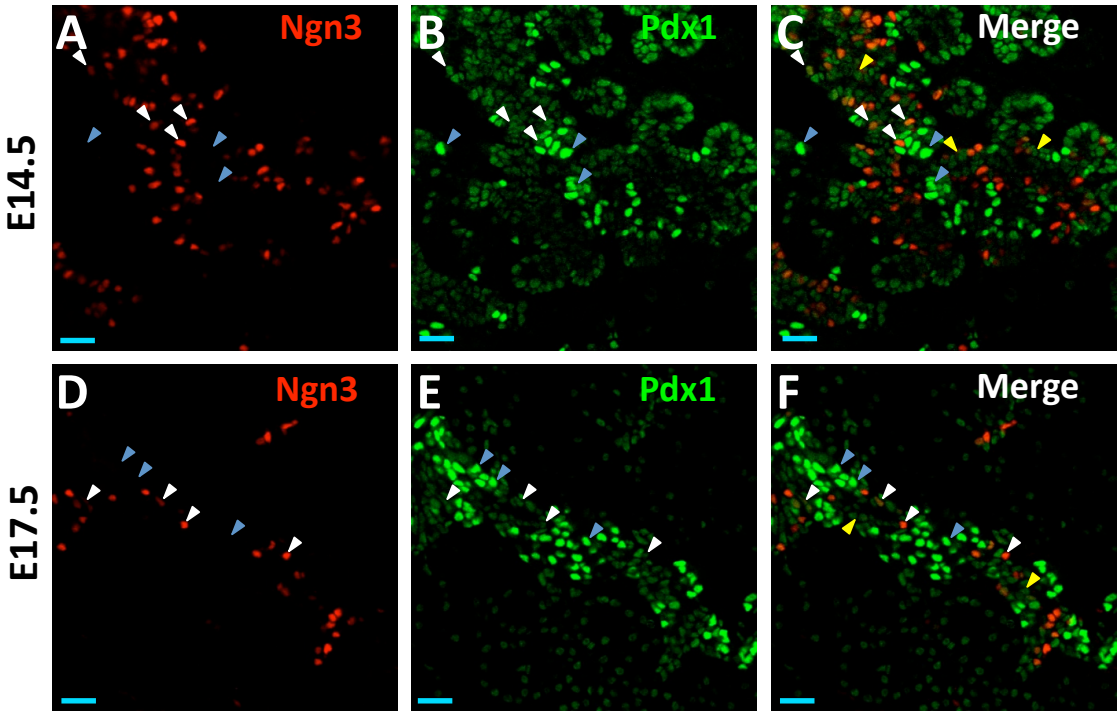

Bankaitis_Supp. Table1

	Sox9^{+} MF	Sox9^{+}Ngn3^{LO}	Sox9^{--}Ngn3^{HI}	Sox9^{--}Ngn3^{LO}
1 hour	76 (n=3)	307 (n=3)	462 (n=3)	227 (n=3)
2 hour	93 (n=3)	234 (n=3)	402 (n=3)	265 (n=3)
3 hour	71 (n=3)	181 (n=2)	259 (n=2)	189 (n=2)
6 hour	74 (n=3)	367 (n=3)	404 (n=3)	235 (n=3)
8 hour	105 (n=3)	445 (n=3)	469 (n=3)	340 (n=3)
10 hour	186 (n=3)	197 (n=2)	387 (n=3)	328 (n=2)
12 hour	90 (n=3)	232 (n=3)	452 (n=3)	216 (n=3)
13 hour	55 (n=3)	391 (n=3)	344 (n=3)	244 (n=3)
15 hour	190 (n=3)	510 (n=3)	719 (n=3)	602 (n=3)
17 hour	142 (n=3)	ND	535 (n=3)	507 (n=3)
19 hour	69 (n=2)	ND	ND	78 (n=2)
22 hour	25 (n =3)	ND	ND	151 (n=3)
24 hour	62 (n=3)	ND	ND	247 (n=3)

Bankaitis_Supp. Fig5

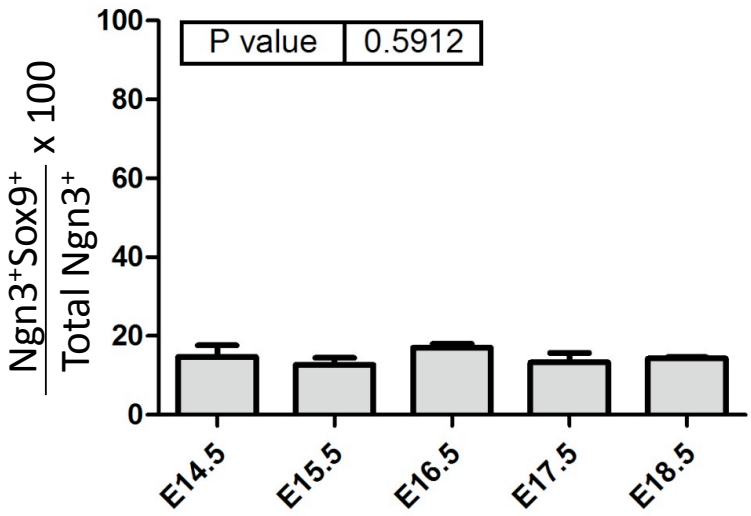

Bankaitis_Supp. Fig6

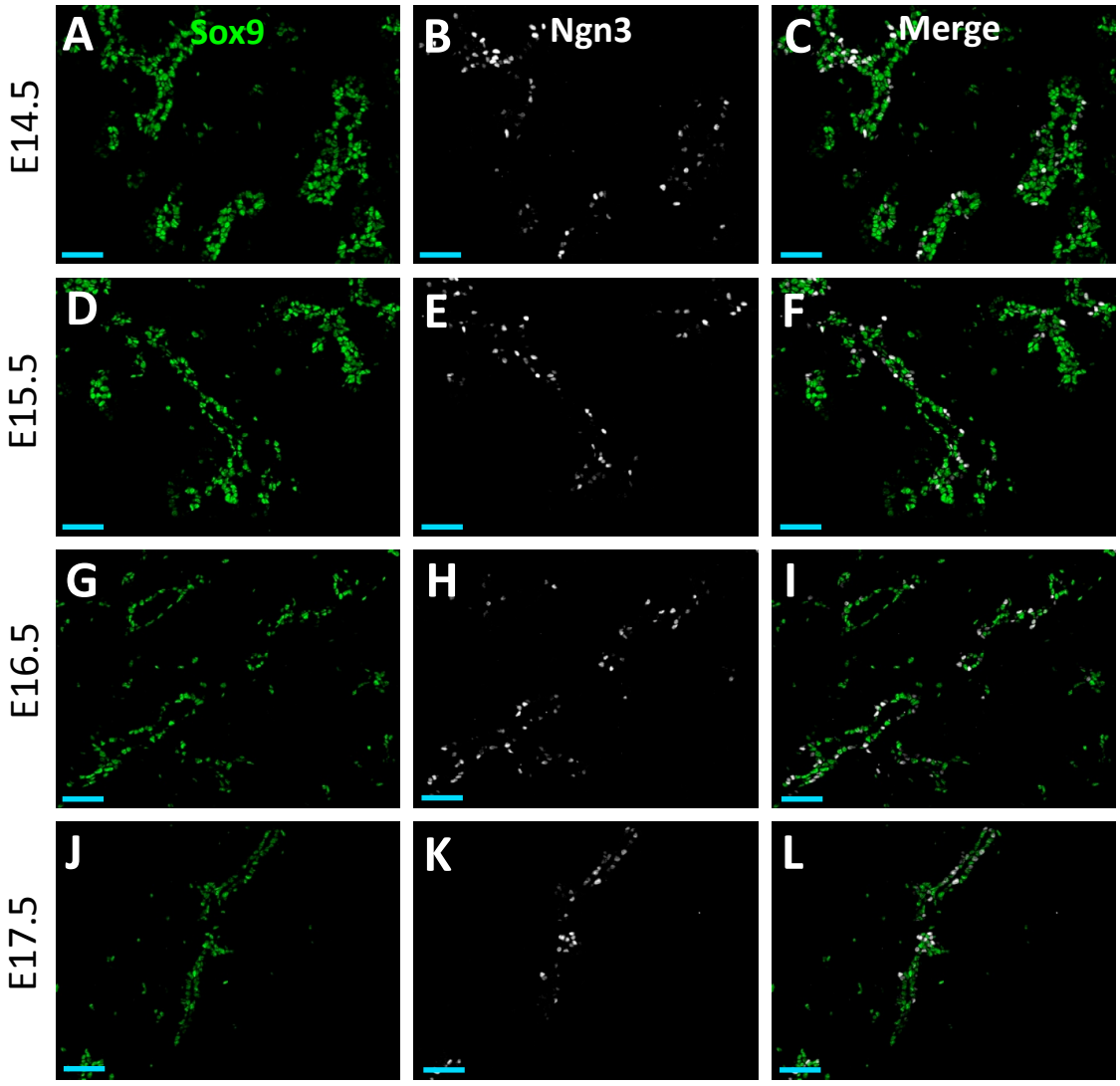

Bankaitis_Supp. Fig7

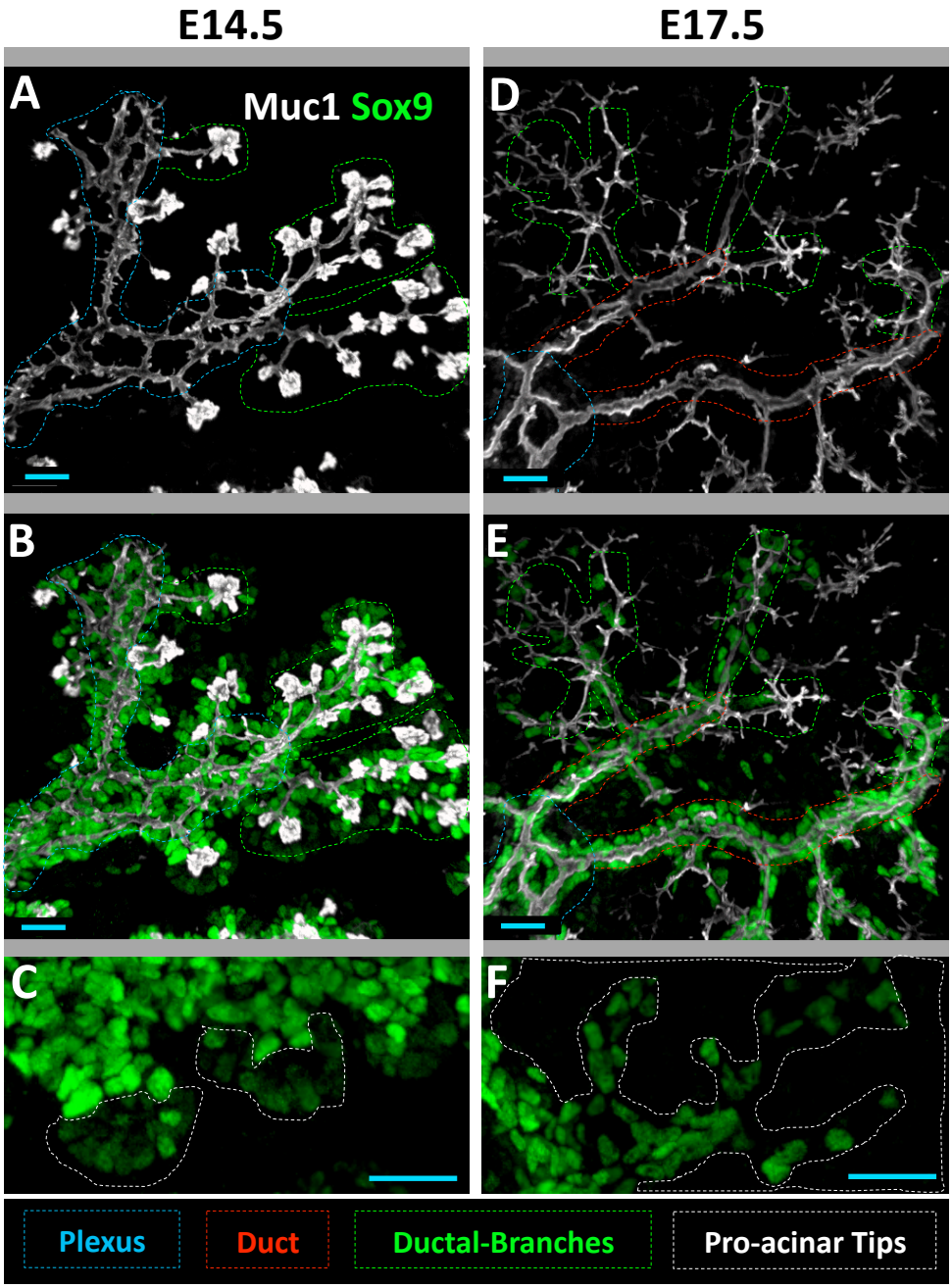

Bankaitis_Supp. Fig8

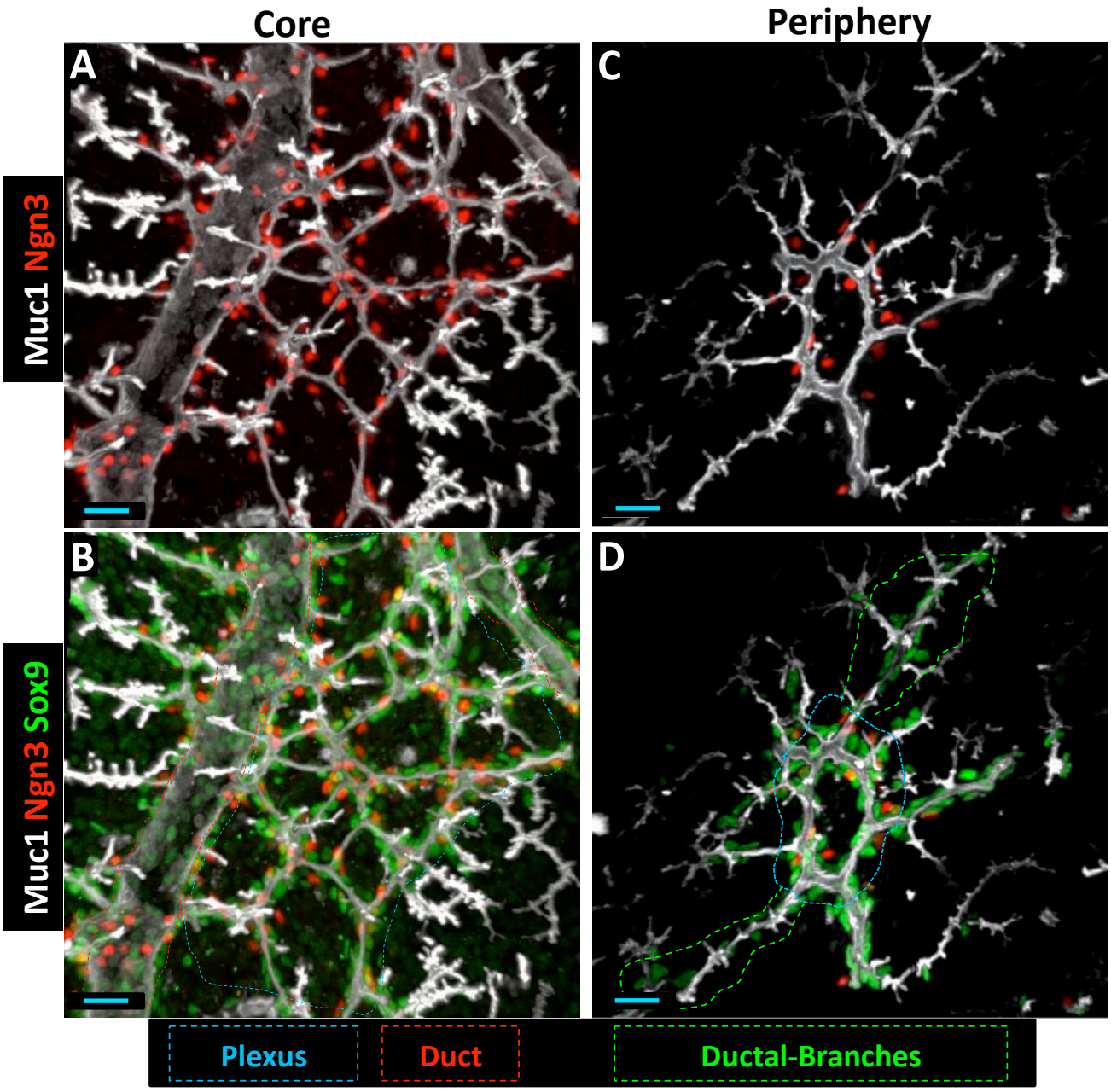

Bankaitis_Supp. Fig9

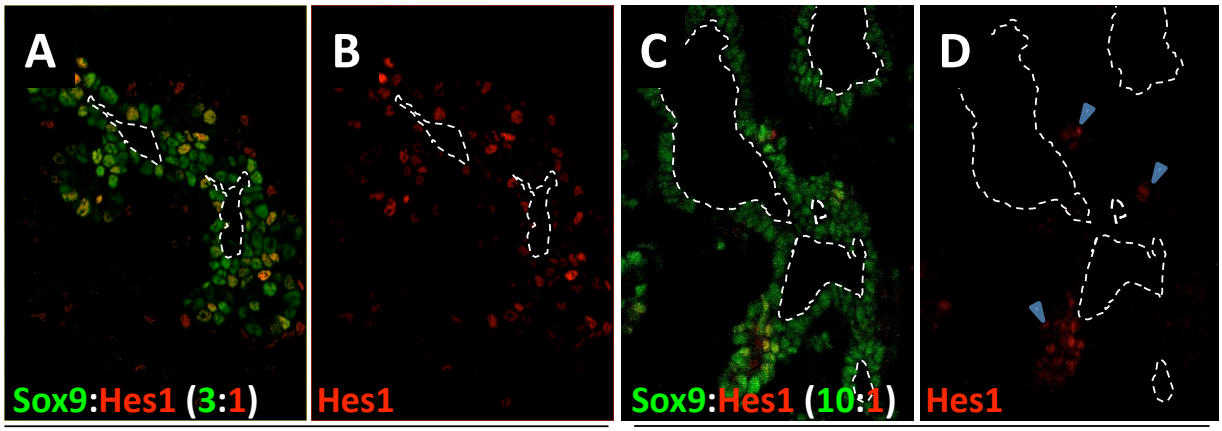

Bankaitis_Supp. Fig10

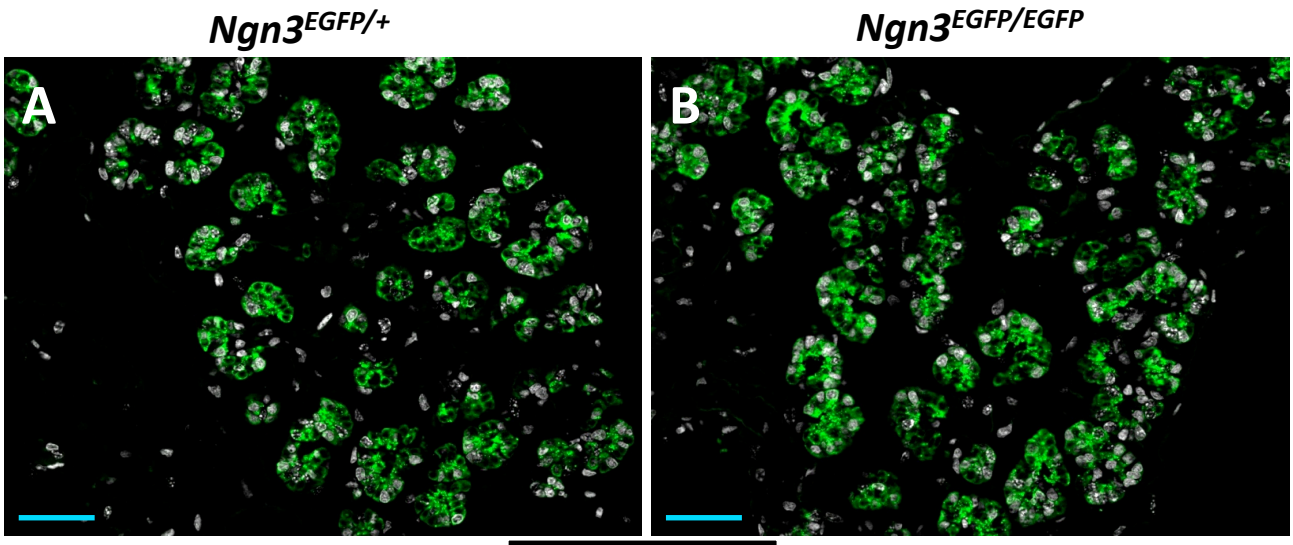

Amylase EdU

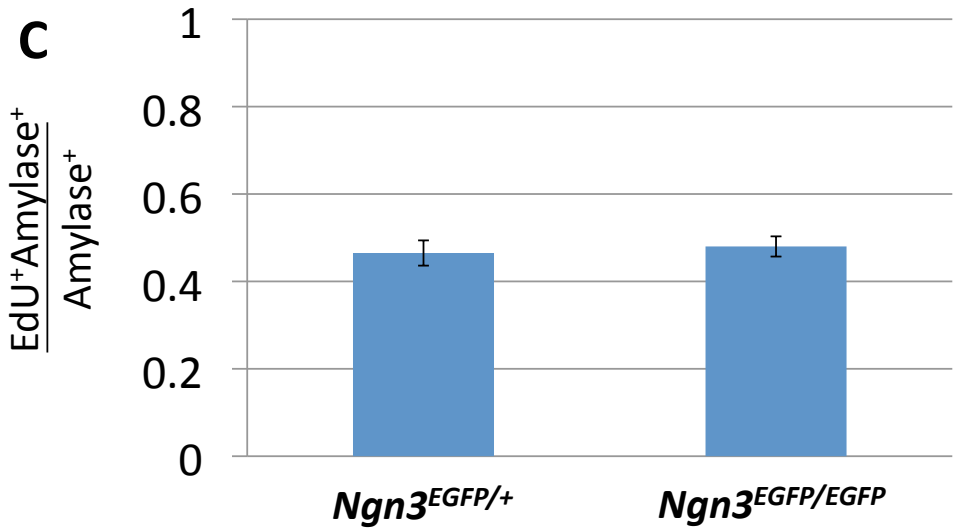

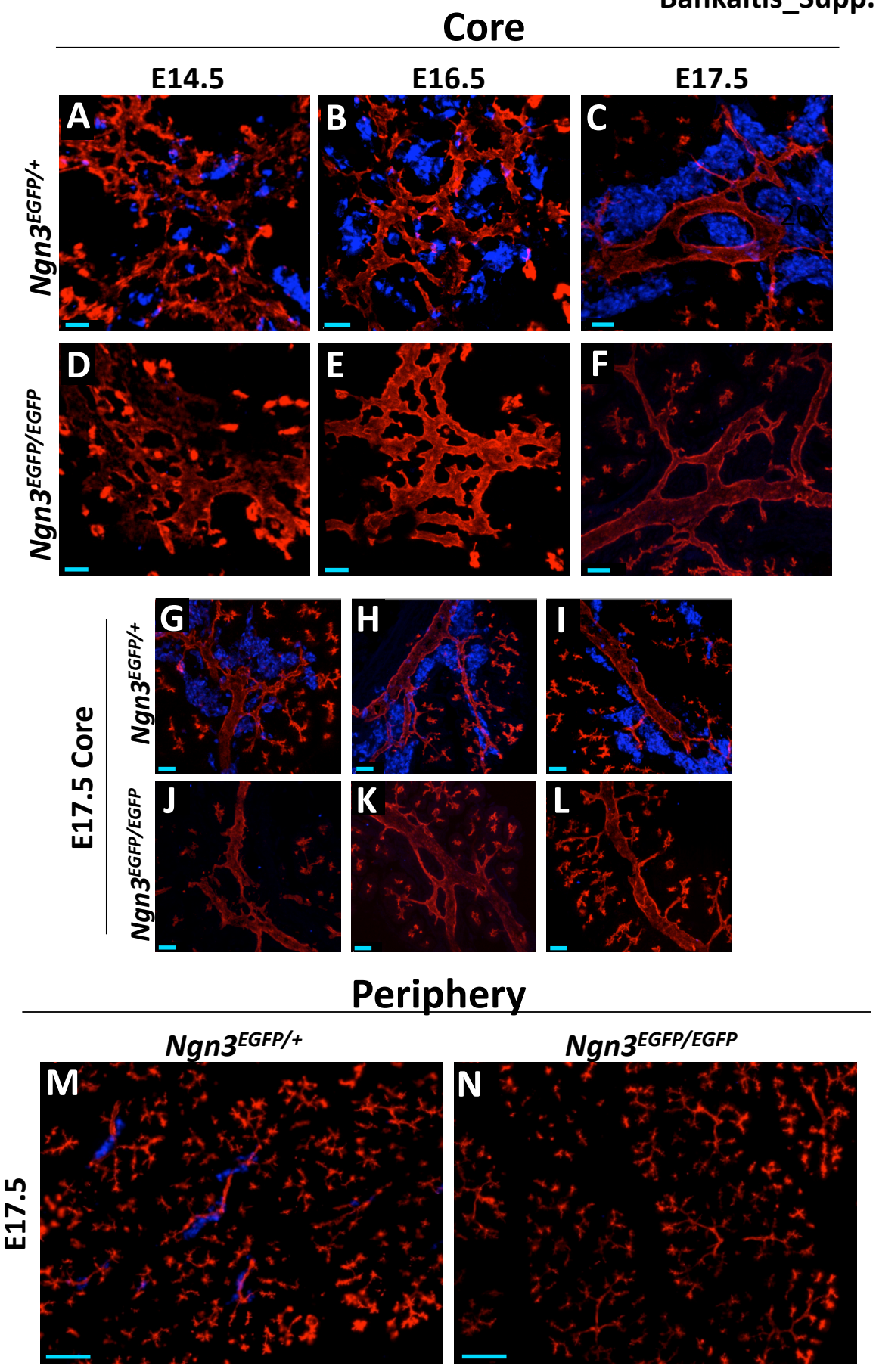
Core
E14.5
E16.5
E17.5
A
B
C
Ngn3EGFP/+
D
E
F
Ngn3EGFP/EGFP
20x
E17.5 Core
G
H
I
Ngn3EGFP/+
J
K
L
Ngn3EGFP/EGFP
Periphery
Ngn3EGFP/+
Ngn3EGFP/EGFP
E17.5
M
N

Bankaitis_Supp. Fig12

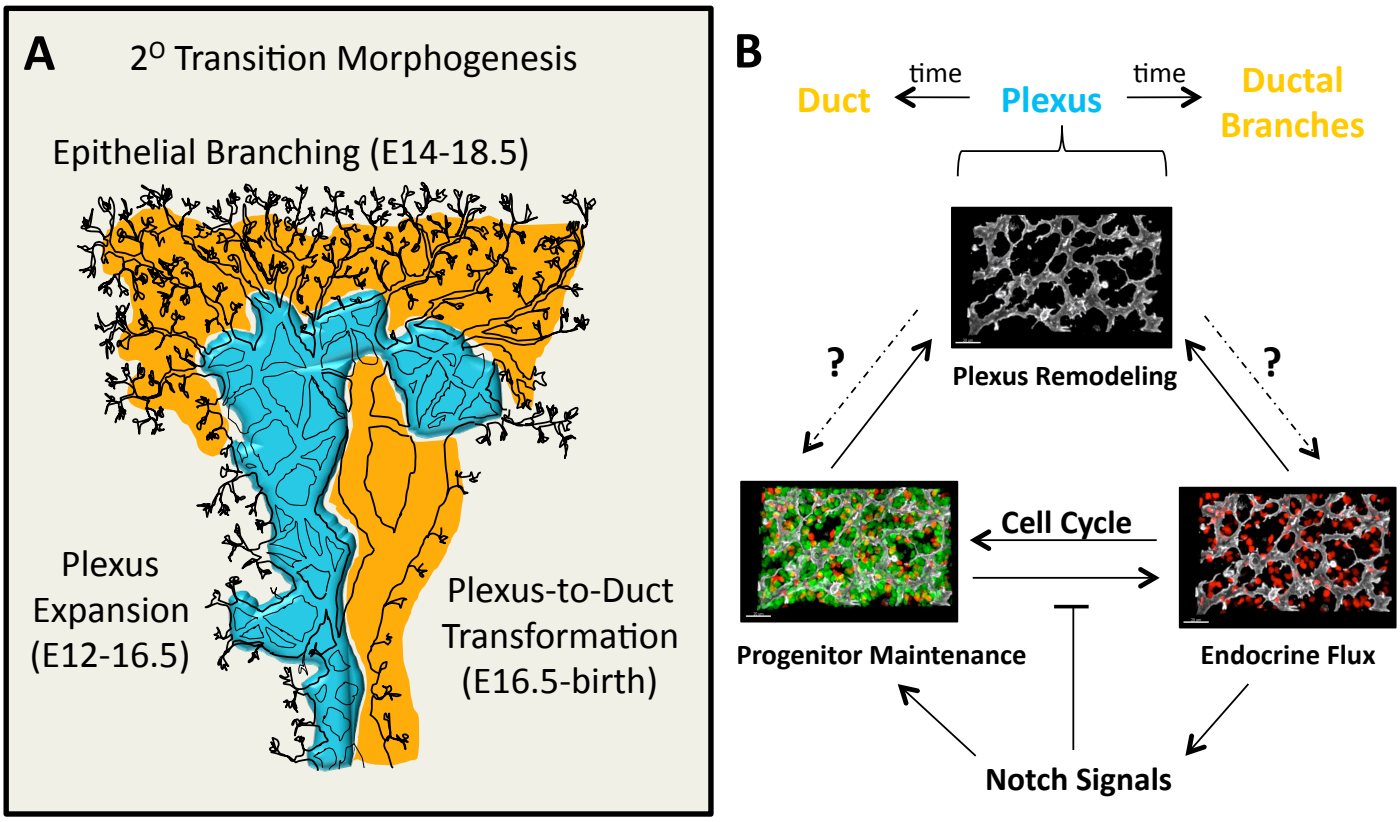

Bankaitis_Supp. Table 2

Primary Antibodies				
Antigen	**Specie**	**Dilution**	**Label Method**	**Source**
Muc1	Hamster	1:1000	IF	NeoMarkers
DBA	Biotinylated	1:400	Direct	Vector Labs
CK19	Rabbit	1:2000	IF	B. Stanger (U. Penn)
Sox9	Rabbit	1:5000	IF	Millipore
Ngn3	Goat Guinea pig	1:40,000 1:2000	Biotin amplify Biotin amplify	G. Gu (Vanderbilt) M. Sander (UCSD)
EdU	----	----	----	Molecular Probes
Pdx1	Guinea pig	1:1000	IF	C. Wright (Vanderbilt)
Ecad	Rat	1:1000	Biotin amplify	AbCam
Hes1	Guinea pig	1:4000	Biotin amplify	T. Sudo (Toray Industries, Japan)
EYFP	Rabbit Chicken	1:2000 1:4000	IF IF	Clonetech Aves
DAPI	----	----	Mount media	Life Technologies
Insulin	Guinea Pig	1:1000	IF	Dako
Amylase	rabbit	1:1000	IF	Sigma

Antigen	Conjugation	Dilution	Source
Guinea pig/Goat/ Hamster/Rat	Cy3/Cy5	1:500	Jackson ImmunoResearch
Rabbit/Chicken	Cy2	1:500	Jackson ImmunoResearch
Rabbit/Hamster	Cy5	1:500	Jackson ImmunoResearch
Goat/Rat	Biotinylated	1:500	Vector Laboratories

Bankaitis_Supp. Table 3

Ngn3EGFP genotyping		
ngn3-1	5’-ATACTCTGGTCCCCCGTG-3’	Lee, 2002
ngn3-2	5’-TGTTTGCTGAGTGCCAACTC-3’	Lee, 2002
EGFP	5’-GAACTTGTGGCCGTTTACGT-3’	Lee, 2002
GAPDH qPCR		
GAPDH 1F	5’-ACTTTGGCATTGTGGAAGG-3’	
GAPDH 1R	5’-GGATGCAGGGATGATGTTCT-3’	
Hes1 qPCR		
Hes1 RTf	5’-TAGCCCACCTCTCTCTTCTGA-3’	
Hes1 RTr	5’-CAGTGCATGGTCAGTCACTTAAT-3’	
Sox9 qPCR		
Sox9 RT2 for	5’-CTCCCCCTTTTCTTTGTTGTTT-3’	
Sox9 RT2 rev	5’-TCTGAAACCTCTCATTTGTCCA-3’	